Heliyon 10 (2024) e31117

Contents lists available at ScienceDirect

Heliyon

journal homepage: www.cell.com/heliyon

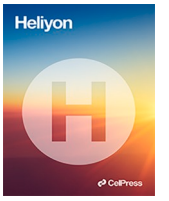

Research article

Characterization of new cellulosic fiber derived from *Lasia spinosa* (L.) thwaites rhizome and its potential use as biodegradable textile material

Methmini Tharanga *, Ujithe Gunasekera

Department of Textile and Apparel Engineering, University of Moratuwa, Moratuwa, Sri Lanka

ARTICLE INFO

Keywords:
Lasia spinosa (L.) thwaites
Scanning electron microscopy
FTIR
X-ray diffraction
Crystallinity index
Tensile strength

ABSTRACT

Fibers extracted from *Lasia spinosa* (L.) thwaites (LS) were characterized to investigate their potential use as biodegradable textile materials. Mechanical and alkali extraction methods were followed to extract LS rhizome fibers. The morphological, physical, chemical, mechanical, and thermal properties of the mechanically extracted rhizome fibers from the commonly available LS species of Lamina-dissected type [LDT] and Sagittate type [SG] were investigated. No previous studies have been done to characterize the LS rhizome fibers. Examination of rhizome fiber morphology using scanning electron microscopy (SEM) revealed that fibers within the dispersed vascular bundles of the rhizome possess a natural crimp.The FTIR result confirmed that the fibers are rich in cellulose. X-RD results confirm a 43 % and 58 % crystallinity index of LDT and SG fibers, respectively, indicating higher amorphous regions and lower crystal phases. Moisture regain of 12.5 % and 14.5 %, single fiber tensile strength of 213.92 MPa and 216.97 MPa, elongation at break of 16.65 % and 17.67 %, and Young's modulus of 1.32 GPa and 1.26 GPa were observed for LDT and SG fibers respectively. Thermogravimetric analysis confirmed thermal stability up to 230 °C for both fiber types confirming their ability to withstand textile processing.

1. Introduction

Today, the textile industry has become one of the leading industries that directly influence the sustainability of the environment due to the manufacturing of larger quantities of non-biodegradable and non-renewable synthetic fibers [1–3]. This has led the research community to investigate biodegradable and renewable sources of fibers in order to reduce the impact of textile manufacturing on the environment, resulting in the proliferation of cellulosic fibers such as cotton, lyocell, and other biodegradable fibers made using soybean plant and polylactic acid (PLA) polymers from cornstarch instead of oil-based synthetic fibers [4].

Characterization of morphological, physiochemical, mechanical, and physical properties of most used textile fibers and several other plant fibers extracted from different parts of the plants, such as *Coccinia grandis* L., stem fiber [5], *Epipremnum aureum*, stem fiber [6], *Juncus effusus* L.,stem fiber [7], *Dichrostachys Cinerea*, bark fiber [8], *Lygeum spartum* L.,stem fibers [9], *Acacia nilotica* L. bark fiber [10], and *Cissus quadrangularis*, root fiber [11], has proven them as probable cellulosic fiber sources for diverse manufacturing applications.

Cellulosic fibers have the potential to be used in the manufacturing of biodegradable textile materials. *Lasia spinosa* (L.) Thwaites

* Corresponding author.
E-mail addresses: methminitr@gmail.com (M. Tharanga), ujithe@uom.lk (U. Gunasekera).

https://doi.org/10.1016/j.heliyon.2024.e31117
Received 22 October 2023; Received in revised form 9 May 2024; Accepted 10 May 2024
Available online 11 May 2024

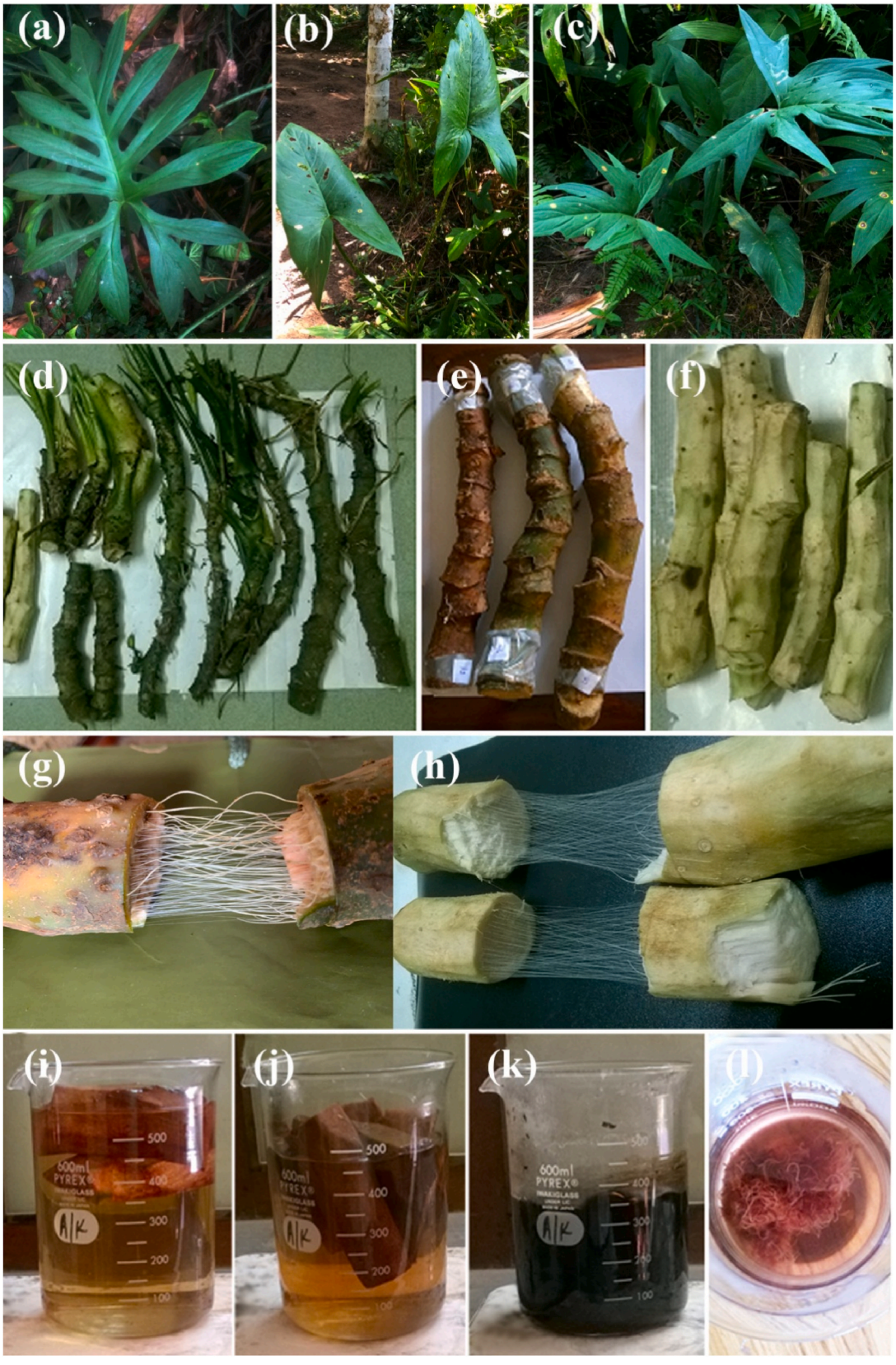

(caption on next page)

Fig. 1. Identified LS types: (a) Lamina-dissected type, (b) Sagittate type, (c) Mixed type, (d) LS rhizome with pointed spines, (e) Rhizomes with pointy spines removed (f) Mud and outer core removed rhizomes, (g) Fibers in matured rhizome, (h) Fibers in immature rhizome, (i), (j) and (k) Rhizomes at different stages with NaOH boiling, (l) Alkali extracted fiber.

(LS) species, which -belong to the monocotyledonous flowering plants and to the Araceae family is distributed in marshy lands in Southeast Asian countries, India, Malaysia, and Sri Lanka [12]. LS is recognized as a herbal plant in Asian countries and in Sri Lankan Ayurvedic medicine. It is considered as a plant that has the potential to be used for a variety of disorders such as colic, rheumatism, depression, anxiety, hemorrhoids, uterine cancer, constipation, injuries, insects and snake bites, skin infections, joint pains, and intestinal disorders [13–18]. Furthermore, rhizomes, leaves, and stems of LS are rich sources of dietary fiber. Lamina-dissected type [LDT], Sagittate type [SG], Mixed type, and Black Lasia are the four main clusters of LS species, which are grouped based on their leaf characters. LDT and SG are commonly available species in Sri Lanka [19].

In this research, the rhizome fiber characteristics of LS plant species were investigated. Mechanical extraction and Alkali extraction techniques were applied in extracting fibers from rhizomes. Morphology, chemical functional groups, crystalline structure, and thermal stability of mechanically extracted rhizome fibers were examined by Scanning electron microscopy (SEM), Fourier transform infrared spectroscopy (FTIR), X-ray diffractometry (XRD) and Thermogravimetric analysis (TGA). Fiber tensile tests were performed to characterize the mechanical properties of fibers. Further testing was carried out to identify the physical behavior of the fibers by measuring moisture absorbency and dye uptake. Characterizations of Alkali-extracted fibers were limited to SEM and FTIR spectroscopy.

2. Material and experimental procedure

2.1. Fiber extraction procedure

Both mechanical and Alkali extraction methods were followed in extracting fibers from rhizomes.

2.1.1. Mechanical extraction

Well-grown rhizomes of LDT and SG plants aged 10 months from their cultivation were collected from farmers in the western province of Sri Lanka. Fig. 1a, b, and c show the leaf characters of the two common species and the mixed-type LS plant, respectively. Initially, the mud and outer layer with pointed spines on rhizomes were removed and washed with distilled water, as shown in Fig. 1d, e, and f. Thereafter, a shallow cut was introduced around the epidermis by a sharp knife. Then the rhizome was split along the cut, and the two parts were separated and gently pulled away from each other. This resulted in the formation of fibers. Further stretching of two rhizome parts enhanced the formation process. Fig. 1g and h depict fiber formation in a mature rhizome and an immature rhizome, respectively.

2.1.2. Alkali extraction

Alkali treatment has been used in extracting fibers from natural resources due to its ability to enhance the mechanical properties of fibers by removing hemicelluloses, pectin, lignin, and impurities from the fiber surface [20]. Cleaned rhizomes were submerged in a 5 % NaOH solution and boiled for 2 h to dissolve the flesh and separate fibers. Separated fibers were washed with warm distilled water, removing the flesh particles, and oven-dried at 60 °C for 12 h [21,22]. Fig. 1i, j, and k present the rhizome at different stages of the extraction process. Separated fiber after washing with warm distilled water is shown in Fig. 1l.

Fibers were conditioned under the standard atmospheric conditions according to ASTM D1776. Accordingly, fibers were kept at a temperature of 21 ± 1 °C and under 65 ± 2 % relative humidity conditions for 8 h.

2.2. Characterization of Lasia spinosa rhizome fiber

2.2.1. Rhizome anatomy of Lasia spinosa

Optical microscope analysis was performed to study the anatomy of the cross-section and the longitudinal section of the rhizome.

2.2.2. Morphological characteristics of LS fiber

The surface morphology of both mechanically extracted and Alkali extracted LS fibers were examined using a light microscope, ZEISS EVO 18, and Hitachi SU6600 research scanning electron microscopes [SEM]. Fibers were sputter coated with a thin gold layer prior to mounting to the SEM. Coated fiber samples were then mounted on aluminum holders and placed inside the vacuum chamber of the SEM for image generation. The SEM monographs were generated at a resolution range of 150 × −15 KX. The cross-sectional analysis of mechanically extracted fibers was conducted using the freeze fracture technique with the application of liquid nitrogen.

2.2.3. Fourier transform infrared (FTIR) analysis

A Bruker Alpha II Fourier Transform Infrared [FTIR] Spectrometer was used to derive the FTIR spectrum of LS fiber in KBr matrix with 28 scans at a resolution of 4 cm^{-1} between the wave number region of 600–4000 cm^{-1}. Mechanically extracted LDT fibers (LDTF) and SG fibers (SGF) were oven dried at 105 °C for 2–4 h and ground into fine powder using a mortar and pestle. Then the powdered fiber was mixed with IR-transparent potassium bromide (KBr) and pelleted to generate a spectrum under standard conditions. The

chemical groups present in both LDT and SG rhizome fibers were identified using the FTIR spectra obtained.

2.2.4. X-ray diffraction (XRD) analysis

Powdered samples of LS plant fibers were subjected to X-Ray diffraction in a Bruker D8 Discover X-Ray Diffractometer to investigate the degree of crystallinity and crystallinity index (CI). The CI of both fiber types was calculated using equation (1) [23].

$$\text{CI } \% = \left(\frac{I_{002} - I_{am}}{I_{002}}\right) \times 100 \tag{1}$$

where I_{002} = the highest intensity of the crystalline region due to lattice diffraction and, I_{am} = the intensity of the scattered peak of the amorphous region.

The crystal size (CS) of the LS fiber was calculated using Sherrer's equation (equation (02)) [24,25]:

$$\text{CS}_{\text{size}} = \frac{\text{K}\lambda}{\beta \cos \theta} \tag{2}$$

where Scherrer's constant $K = 0.9$, the wavelength of the radiation $\lambda = 1.54$Å [0.154 nm],° β is the peak's full width at half maximum [FWHM] while θ is the diffraction angle.

2.2.5. Moisture relationship analysis

Fiber samples were tested as per the ASTM D2495 -07 test method. A known weight of the conditioned fiber samples was subjected to drying, cooling, and weighing at 1 h intervals until the change in mass between two successive weightings was less than 0.1 % of the sample mass. The moisture content of the fiber samples was measured using equation (3) [5]:

$$\text{Moisture Content } \% = \left(\frac{M - D}{M}\right) \times 100 \tag{3}$$

where M = Original mass of fiber sample in grams (g), D = Oven-dry mass of fiber sample in grams. Moisture regain of the fiber samples were measured using equation (4) [26]:

$$\text{Moisture Regain } \% = \left(\frac{M - D}{D}\right) \times 100 \tag{4}$$

where D = Oven-dry mass of the fiber sample in grams. The mean value of the moisture content and moisture regain was calculated for accurate results.

2.2.6. Fiber tensile properties

ASTM D3822-14 is preferred to determine the tensile strength of a single fiber in the INSTRON 4301 universal tester. ASTM D 1577–07 is preferred to determine the linear density of fibers. Tensile strength, breaking strength and Young's modulus of thirty fiber samples from each fiber type were tested and the mean was calculated.

Tensile strength, breaking elongation and Young's modulus of both fiber types were calculated using equations (5)–(7) respectively [8,11,21].

$$\text{Tensile Strength} = \frac{F_{at\ break}}{\sigma\,(tex)} \tag{5}$$

$$\text{Breaking Elongation} = \left(\frac{\Delta L}{L}\right) \times 100 \tag{6}$$

$$\text{Young's Modulus} = \frac{\frac{F_{at\ break}}{\sigma\ (tex)}}{\left(\frac{\Delta L}{L}\right)} \tag{7}$$

where $F_{at\ break}$ = Force at break, $\sigma\,(tex)$ = Linear Density (tex), L = initial length of the fiber in millimeters, and ΔL = change in length in millimeters due to the application of force.

2.2.7. Dye uptake behavior analysis

Dye uptake was investigated by analyzing scoured and bleached mats of LS rhizome fibers.

The colour strength (K/S) of both LDTF and SGF mats and the cotton textile samples dyed in the same dye bath were calculated using the Kubelka – Munk theory and equation (8) mentioned below [27–29]:

$$\text{K} \Big/ \text{S} = \frac{(1 - R)^2}{2R} \tag{8}$$

where K = Absorption Coefficient, S = Scattering Coefficient, R = reflectance value The obtained colour strength values were compared with the colour strength values of cotton textile material.

2.2.8. Thermogravimetric analysis

Thermal stability determines the aptness of fiber for high-temperature processing and use. The thermogravimetric analysis of both LDTF and SGF was carried out using a SDTQ600 Thermogravimetric Analyzer. The spectrum was recorded within the temperature range of ambient to 800 °C under a high-purity nitrogen gas atmosphere at a heating rate of 10 °C/min.

3. Results and discussion

3.1. Rhizome anatomy analysis

In Fig. 2a and b, the rhizome's cross section and the longitudinal section are illustrated respectively, displaying approximately 100–120 scattered vascular bundles (VB), while the longitudinal section reveals vertically oriented vascular bundles along the vertical axis. The presence of fibrovascular bundles is clearly visible in micrographs of the transverse sections of LDT and SG rhizomes in Fig. 2c and d, respectively, each with a xylem, phloem and fiber bundle [9,11].

3.1.1. Scanning electron microscope analysis

The SEM micrographs in Fig. 3a–g presents the morphology of mechanically extracted LDTF and SGF. In Fig. 3a and b, micrographs illustrate the smallest observable fibers for the naked eye in both plant types. The images depict that the rhizome fibers of both plants exhibit a comparable morphology, featuring cylindrical-shaped fibrils arranged in a helical manner along the fiber axis. Helices observed in nature are the secondary structure found in polysaccharides [30]. Fig. 3c displays inherently crimped 16–25 fibrils in a single fiber strand. This remarkable characteristic is evident in plant fibers -in contrast with the predominantly utilized natural fibers in the textile manufacturing industry.According to Fig. 3d and e, the diameters of fibrils lie within a range of 2.5 μm–6.5 μm in both plant types. These fibrils appear to have bonded together in a random manner. Bonds between fibers are usually formed with the involvement of pectin and non-cellulosic substances [31]. The cross-section of LDT and SG fibrils is presented in Fig. 3f and g respectively. The shape of the fibril cross section seems rounded to polygonal; however, the inconsistency of the diameter along the fiber length results in the cross sectional size varying. The cell formation of the inner structure of the fibril in both fiber types shows that it has porous areas in between the cell walls. Inherent crimping was observed on both LDTF and SGF as shown in Fig. 3h and i. The primary wall of the fibril is visible to the outside, with several other secondary walls forming towards the middle of the fibril. Fibers

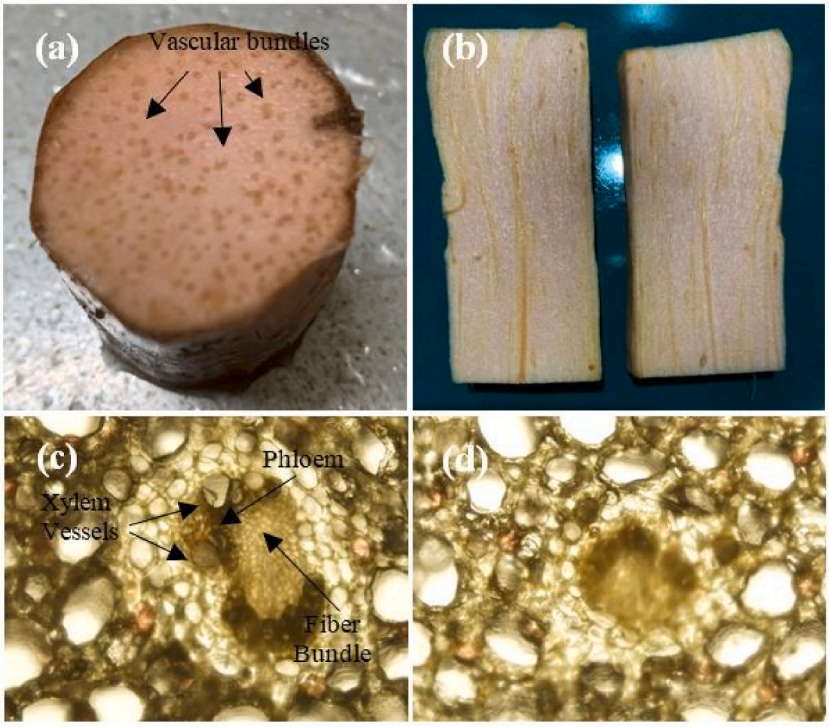

Fig. 2. Naked eye view of (a) rhizome cross section, (b) rhizome longitudinal section, (c) micrograph of the transverse section of LDT rhizome 10x, (d) micrograph of the transverse section of SG rhizome 10x

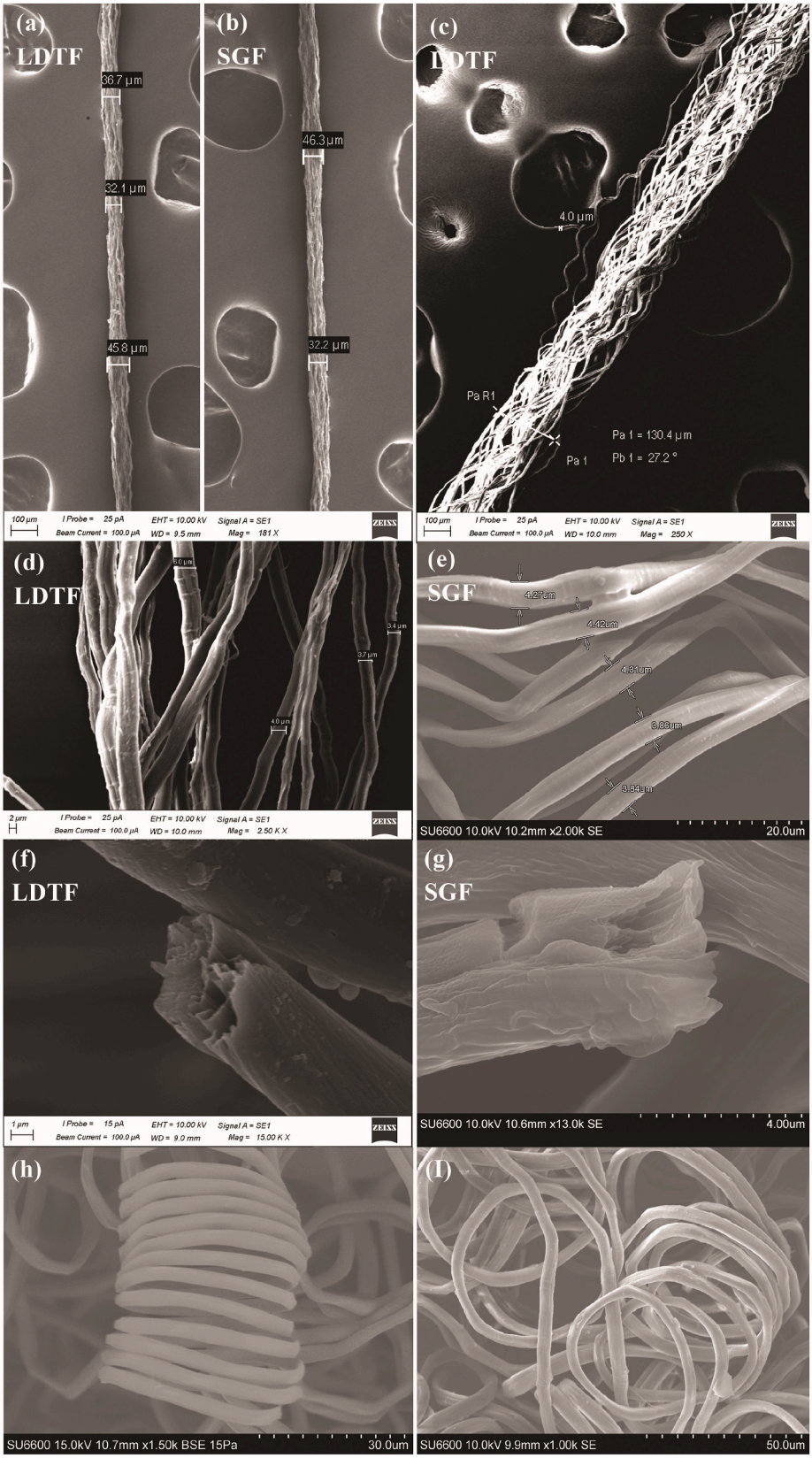

(caption on next page)

Fig. 3. SEM micrographs of LS fiber: (a) and (b) LDTF and SGF at 181X, (c) LDTF at 250X, (D) LDTF at 2.50KX and (e) SGF at 2.00K, (f) cross-section of LDTF at 15KX, (g) cross section SGF at 13K, (h) and (i) crimp on LDTF and SGF.

were found to be stretchable due to their high crimp. Fig. 4a and b depict the surface morphology of mechanically extracted and alkali extracted fibers, respectively. Mechanically extracted fiber surfaces look rough and uneven due to cavities with small voids, contaminated pectin, lignin, oil, and impurities [5,11], whereas alkali-extracted fiber surfaces show the absence of contaminants on the surface of the fiber. With this result, it is evident that the alkalization modifies the surface of fibers.

Micrographs of thicker fibers found in rhizomes are shown in Fig. 4c and d, with diameters ranging from 318 μm to 350 μm. A higher number of cavities with voids and other contaminants appeared on the surface of the fiber. A high number of high-density fibers are found in mature rhizomes. This is possible due to the starch deposition and lignification processes of plant cells, which increase with the maturity of plants [32].

3.2. FTIR analysis

The FTIR spectra of LDTF and SGF are shown in Fig. 5a and b. Both spectra look similar to each other, but varied transmission values were observed in the same wave range. In the FTIR spectrum, the absorption bands associated with IR vibrations indicate various molecular activities, including stretching, bending, or wagging of the chemical groups present in fibers.

The broad peaks observed at 3383 cm^{-1} in LDTF and 3360 cm^{-1} in SGF are associated with the O–H stretching of the hydroxyl groups [33] confirming the presence of alpha cellulose in both fiber types [5,6,11]. The peak observed at 2918 cm^{-1} on both LTDF and SGF is attributed to C–H stretching of cellulose [5–7,9,11,24]. The peak observed at 2362 cm^{-1} of LDTF attributes to the C ≡ C stretching of waxes presented in fibers [5]. The absorption band recorded at 1737 cm^{-1} on both LDTF and SGF relates to C = O stretching of hemicelluloses [5], [6]. Peaks correspond to the C = O stretching observed at 1634 cm^{-1} in LDTF and at 1635 cm^{-1} in SGF. The presence of lignin in both fibers confirms the C = C stretching peak observed at 1510 cm^{-1}. The peak indicates CH_2 symmetric bending resulted at 1425 cm^{-1} wavelength, confirming the presence of cellulose in both LDTF and SGF. The wave numbers of 1376 cm^{-1} of LDTF and 1374 cm^{-1} of SGF are attributed to the C–H stretching of cellulose. Peaks at 1254 cm^{-1} of LDTF and 1252 cm^{-1} of SGF are associated with C–O stretching of acetyl groups in lignin. Both the fiber types presented a peak at 1159 cm^{-1} which corresponds to the C–O–C stretching of cellulose and hemicelluloses. Very clear peaks occurred at 1051 cm^{-1} of LDTF and 1052 cm^{-1} of SGF, indicating the C–O stretching of hydroxyl and ether groups in cellulose [7,9]. The results confirm the existence of cellulose, hemicelluloses, and lignin in the longitudinal section (LS) of plant rhizome fibers.

3.3. XRD analysis

Fig. 6a and b presents the X-Ray diffraction patterns for LDTF and SGF respectively. Peaks recorded are attributed to the presence of cellulose type I in both fibers which is known as native cellulose. I_{002}, the highest intensity at $2\theta = 22.64^{\circ}$ for LDTF and $2\theta = 21.95^{\circ}$ for

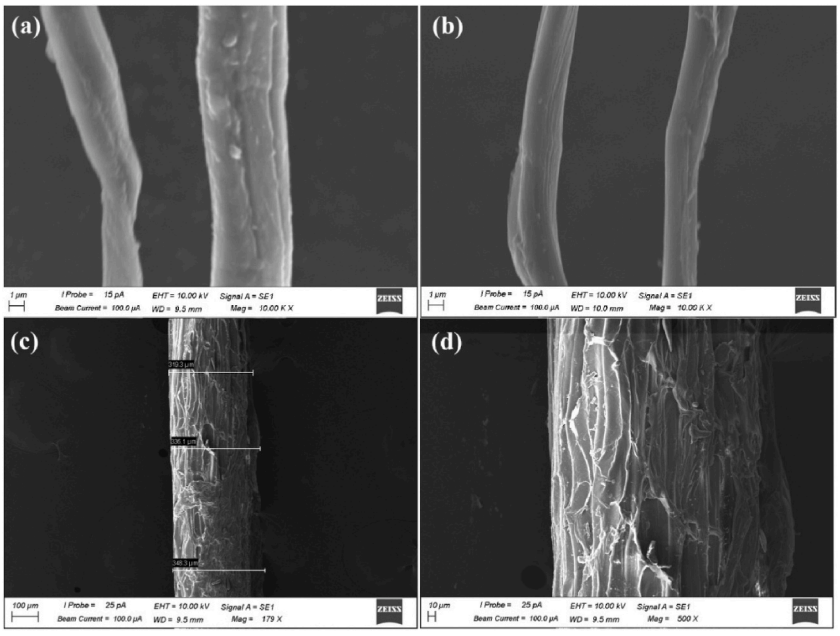

Fig. 4. SEM micrographs of LS fiber (a) contaminants on hand extracted fiber surface, (b) NaOH extracted fiber, (c) matured fiber at 179X, (d) matured fiber at 500X

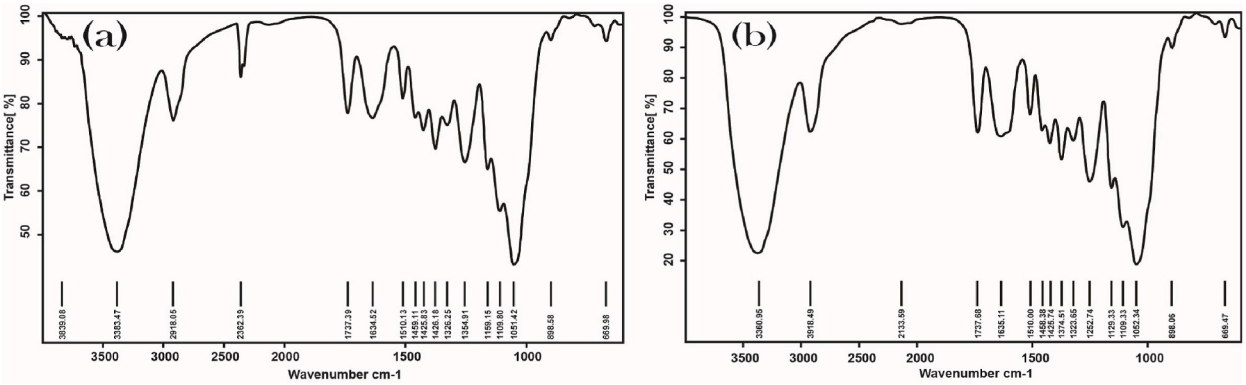

Fig. 5. FTIR graphs: (a) LDTF and (b) SGF.

SGF, corresponds to the intensity peak of the crystalline region due to lattice diffraction, and I_{am}, the lowest intensity at $2\theta = 17.18^{\circ}$ for LDTF and $2\theta = 17.02^{\circ}$ for SGF, corresponds to the intensity scattered peak of the amorphous region. Amorphous phases in cellulose, hemicelluloses, and lignin contribute to the poor peaks of diffraction [7]. A crystallinity index (CI) of 43 % and 58 % was obtained for LDTF and SGF, respectively. The crystallinity index of LDTF and SGF is higher than that of *Juncus effusus* L. (33.4 %) [7], *Wrightia spartum* L.stem fiber (40.6 %) [34], Grewia tiliifolia (41.7 %) [35], and G. damine stem bark fiber (30.35 %) [36], and it is lower than cotton (60 %) [24], lotus (52 %) [37], Epipremnum aureum (49.33 %) [6], *Coccinia grandis*.L (52.17 %) [5], *Cissus quadrangularis* (56.6 %) [11], *Althea Officinalis* L. (65 %) [21], Date Palm rachis (47.80 %) [33] and *Lygeum spartum* L. (46.19 %) [9].

The crystalline sizes of 1.28 nm and 1.29 nm were obtained for LDTF and SGF, respectively. The CS of the LS fiber is lower than that of cotton (5.5 nm) [7], lotus stem (2.5 nm) [37], and *Juncus effusus* L. (3.6 nm) [7] fibers. Fibers with a fewer degree of crystallinity have lower crystal regions but more amorphous regions [37]. The CI value of 43 % reflects that the LS rhizome fiber consists of highly amorphous regions compared to crystalline regions.

3.4. Moisture regain analysis

Moisture contents of 11.4 % and 12.6 % were obtained for LDTF and SGF, respectively. The moisture regain values for LDTF and SGF are recorded as 12.5 % and 14.5 %, respectively.Moisture absorbency values of LS rhizome fibers are comparatively higher than those of cotton and lotus fiber [38]. Low crystallinity index (CI) and crystalline size suggest the prevalence of substantial amorphous regions within the fiber. Cellulose in the amorphous regions interacts with water molecules when fibers are open to moisture. High moisture absorbency results due to the hydrophilic nature of the carbohydrates. The nature of swelling increases with the volume of fiber due to the liquid uptake observed in LS fiber [39]. Table 1 presents the physical properties of LS fibers and most commonly used textile fibers in manufacturing textiles.

3.5. Tensile test analysis

During the tensile testing of fibers, uncrimping of fiber at initial force application, deformation of the fiber molecule structure, yield point, and sudden drop at the breaking point are observed. Elongation at the beginning of the deformation stage is due to the stretching and shearing of the primary and secondary bonds of the amorphous phases [41]. Fig. 7a presents the stress-strain curves of 3 selected LTD and SGF fiber specimens. All 6 fibers' stress-strain curves behave non-linearly under tensile testing until they break. It is noteworthy that both fibers have comparable mechanical properties.

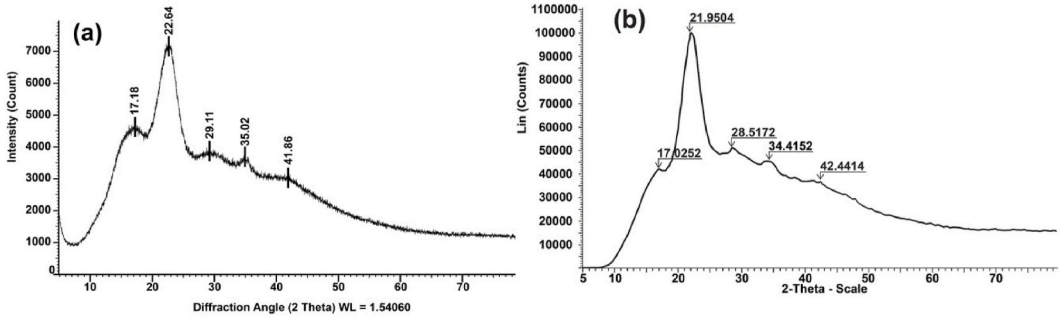

Fig. 6. XRD graphs: (a) LDTF and (b) SGF.

Table 1
Comparison of physical properties of LS fiber with other cellulosic fibers.

Fiber type	Moisture content (%)	Moisture regain (%)	Crystallinity Index (%)	Crystal size (nm)	Reference
Lasia spinosa LDTF	11.4	12.5	43	1.28	
Lasia spinosa SGF	12.6	14.5	58	1.29	
Cotton	7.34	8.5	60	5.5	[7]
Flax	3.9	–	80	2.8	[11]
Sisal	11.1	–	55	16.9	[40]
Lotus	–	12.3	52	2.5	[37]
Kenaf	6.2–12	–	–	–	[40]
Jute	12.5–13.7	71	–	–	[40]
Hemp	6.2–12	–	–	–	[40]

The tensile strength of LDTF is found as 213.92 MPa and that of SGF is 216.97 MPa.The standard deviation of tensile strength of LDTF and SGF are 12.35 MPa and 14.37 MPa respectively. LS fiber tensile strength is lower than the tensile strength of cotton 400 MPa, flax 500–1500 MPa, jute 393–773 MPa, banana 529–759 MPa, *Cissus quadrangularis* 1857–5330 MPa [11], *Lygeum spartum* L.280 MPa [9], *Coccinia grandis*.L. 273 ± 27.74 MPa, *Althaea officinalis* L. 415.2 MPa [5] and also to the *Epipremnum aureum* stem 317–810 MPa [6] which is from the same plant family that the LS belongs to and is higher than Pineapple leaf fiber 126.6 MPa [42] and *Juncus effusus* L. 113 ± 36 MPa [7].

The elongation at break obtained for LDTF and SGF is 16.65 % and 17.67 % respectively. The LS fiber elongation at break is outstanding in comparison to the elongation values of cotton 7–8%, *Cissus quadrangularis* - root 3.57–8.37 %, bamboo 1.4 %, banana 1–3.5 % [11], jute – stem 1.15–1.5 %, hemp – bast 2.2 % [7] and *Epipremnum aureum* stem 1.38–4.2 % [6]. Inherent crimp observed in SEM images of the LS fiber confirms the correlation between crimp release and higher elongation of fibers. Further, high amorphous content compared to crystalline regions results in a higher extension percentage of fibers [41]. Young's modulus for LDTF and SGF is 1.32 GPa and 1.26 GPa with the standard deviation of 0.24 GPa and 0.22 GPa respectively. The obtained Young's modulus value for LS fiber is lower than that of cotton (5–12 GPa), *Cissus quadrangularis* (68–203 GPa) [11], flax (52.5 ± 8.6 GPa), jute (1.3–42.2 GPa) [7] and *Epipremnum aureum* (8.41–69.61 GPa) [6]. These results emphatically indicate that the morphological formations of fibers are the reason for their tensile properties. Table 2 shows the mechanical properties of commonly used fibers for textiles and different other plant fibers characterized for composite materials that may have the potential to be used for biodegradable textile manufacturing.

The tensile strength fluctuation of brittle materials is commonly depicted by the application of the Weibull probability distribution [5,7,33,46].Fig. 7b, c and d demonstrate the two-parameter Weibull distribution for LDTF and SGF with a confidence level of 95 %. Tensile strength, elongation at break, and Young's modulus for LDTF are 219.7 MPa, 17.6 %, 1.42 GPa and for SGF 223.6 MPa, 18.96 %, 1.35 GPa respectively. From these values it can be clearly observed that the tested values are almost similar to the values obtained through the Weibull analysis.

3.6. Dye up-take behavior analysis

Fig. 8a graph presents the light reflectance (R) values at the maximum wavelength of absorbency (λ maximum) of the dyed fiber mattes of LDTF and SGF as 73.79 and 73.58 respectively. Fig. 8b and c presents the raw fiber matt weaving manually using a frame loom and the woven raw fiber matt in that order. Woven LS fiber matt and a piece of cotton textile were dyed to compare the colour strength of the LS fibers. Fig. 8d and e depict the dyed LS fiber matt and the dyed cotton textile correspondingly. The colour strength (K/S) values of LDTF and SGF are 35.9 and.

35.8 respectively. Compared to the cotton fiber colour strength of 41.8 [47], LS fiber has slightly less colour strength than cotton fiber. This behavior is contrary to the common knowledge that low crystalline structures have higher colour strength. The lower dye uptake of LS fibers compared to cotton may be due to the presence of lignin and other non-cellulosic material in LS fiber.

3.7. Thermogravimetric analysis

Fig. 9a and b presents the thermogravimetric (TG) and its derivative thermogravimetric (DTG) curves obtained for the LDTF and SGF respectively. According to the curves, initial weight loss of 12.71 % for LDTF and 9.11 % for SGF is recorded between room temperature and 100 °C, corresponding to the vaporization of water presented in the fiber [6]. After the initial mass loss it is observed a thermal stability from 100 °C to 230 °C on both the fibers. The second mass loss is observed between 230 °C to 340 °C. These results correspond to the glycosidic linkages of cellulose and breakdown of hemicelluloses in fiber [5,6,11,21].

The derivative thermogravimetry (DTG) curves show clear peaks at 329.43 °C for LDTF and 332.03 °C for SGF, which is the decomposition peak temperature resulting due to thermal decomposition of cellulose I and complete decomposition of ∞ cellulose. Similar peaks are recorded in the literature for several natural fibers such as Bamboo, Hemp, Jute, and Kenaf fibers at 321 °C, 308.2 °C, 298.2 °C and 307.2 °C respectively [11]. The third stage of the TG spectrum indicates the degradation of wax and lignin in the fiber within the temperature range of 340 °C - 540 °C [11,48], and [5]. According to the FTIR analysis, it is found that the LS rhizome fiber consists of small quantities of lignin and waxes. Thus, the weight loss recorded in the spectrum of LDTF is attributed to the degradation of wax and lignin in the LS fiber. At temperatures above 500 °C the molecules of the fiber will breakdown into CO_2, CO, H_2O, hydrocarbons and hydrogen which are low molecular weight products [11]. The results of the thermal analysis of both fiber types

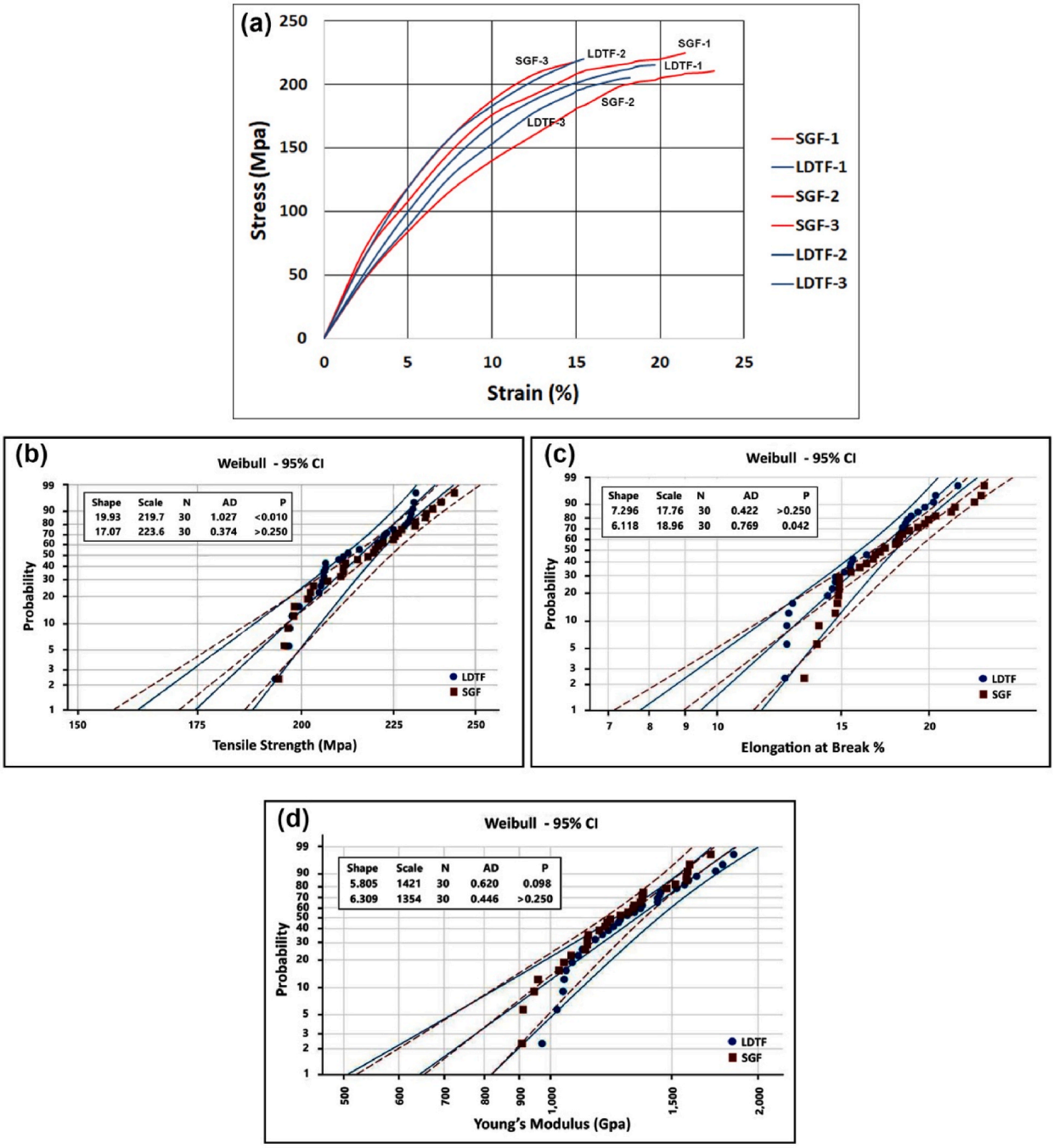

Fig. 7. (a) Stress-strain curves of 3 fiber samples in each LDTF and SGF, Two-parameter Weibull distribution for LDTF and SGF for (b) tensile strength (c) elongation at break (d) Young's modulus.

indicate that the raw LS fiber has.

thermal stability up to 230 °C indicating that the LS fiber can withstand most of the textile process conditions and is possible to use in the manufacture of composites.

4. Conclusions

In this investigation, the rhizome fibers of the two commonly found species of *Lasia spinosa* (L.) Thwaites (LS) plants were characterized to assess the potential use of fiber for biodegradable textile material. The results obtained led to the following conclusions:

Table 2
Comparison of mechanical properties of LS fiber with other cellulosic fibers.

Fiber type	Tensile strength (MPa)	Elongation (%)	Young's modulus (GPa)	Reference
Lasia spinosa LDTF	213.92	17	1.32	
Lasia spinosa SGF	216.97	18	1.26	
Cotton	300–700	7–8	5–13	[11]
Flax	865.9	2.09	40.78	[43]
Jute	393–773	1.5–1.8	26	[11]
Hemp	262.68	1.47	22.44	[43]
Banana	529–759	1–3.5	8	[11]
Bamboo	503	1.4	35.91	[11]
Sisal	274–526	1.8–7.7	6.7–21.7	[9]
Kenaf	295–930	1.6–6.9	53	[44]
Pineapple leaf fiber	630 ± 50	7.9 ± 0.7	9 ± 1.1	[45]
Cissus quadrangularis	1857–5330	3.57–8.37	68–203	[11]
Lygeum spartum L.	280	1.49–3.74	4.47–13.27	[9]
*Coccinia grandis.*L.	273 ± 27.74	2.70 ± 0.27	10.17 ± 1.261	[5]
Althaea officinalis L.	415.2	3.9 9	65.4	[5]
Epipremnum aureum	317–810	1.38–4.2	8.41–69.61	[6]
Juncus effusus L.	113 ± 36	2.75 ± 0.68	4.38 ± 1.37	[7]

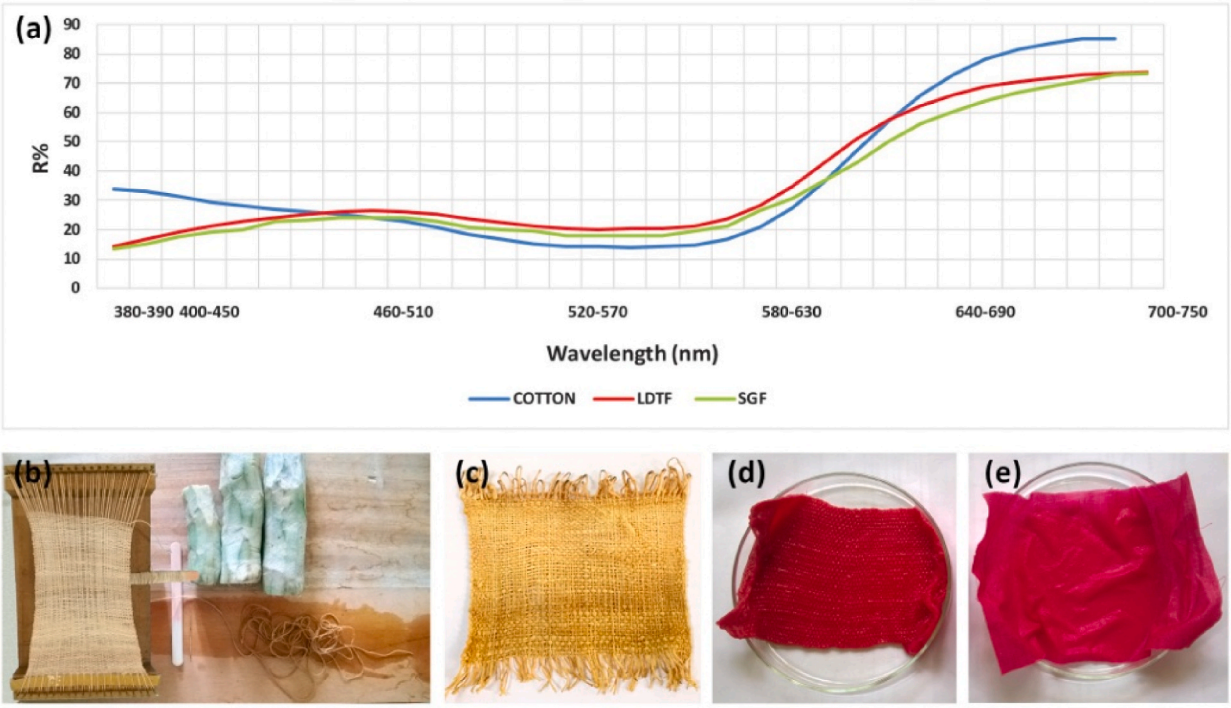

Fig. 8. (a) Light reflectance (R) values vs wavelength of LDTF, SGF and Cotton, (b) and (c) LS rhizome fiber matt sample, (d) dyed LS matt, (e) dyed cotton textile.

Inherently crimped fibrils observed with a diameter ranging from 2.5 μm to 6.5 μm through the SEM confirm the stretchability perceived on LS fibers. Further study of this property of fibers might lead to biomimicking ideas to innovate stretchable cellulosic fibers that support circularity.The FTIR analysis of fiber from both plant types confirmed that the LS plant rhizome fibers consist of cellulose, hemicelluloses, lignin, and a small amount of wax. The crystallinity index of 43 % and the crystalline size of 1.28 nm obtained from the X-RD analysis for LDTF confirmed the presence of a higher amorphous percentage and a low crystal percentage in LDTF fibers. The crystallinity index (CI) of 58 % and the crystalline size of 1.29 nm resulted in SGF, confirming the opposite representation of amorphous and crystal regions in SGF to LDTF.The moisture regain and moisture content values of LDTF and SGF showed slight differences, resulting in 12.54 % and 11.14 % for LDTF and 14.5 % and 12.63 % for SGF, respectively. This result indicates that the LS fiber has higher moisture absorbency which emphasize its suitability for textile application. The tensile strengths of LDTF and SGF are 213.92 MPa and 216.97 MPa respectively. The very high breaking elongation of LDTF and SGF confirms with 16.89 % and 16.94 %, respectively. Young's modulus for LS fiber is 1.3 GPa, which indicates higher extensibility at small extensions.The dye uptake behavior

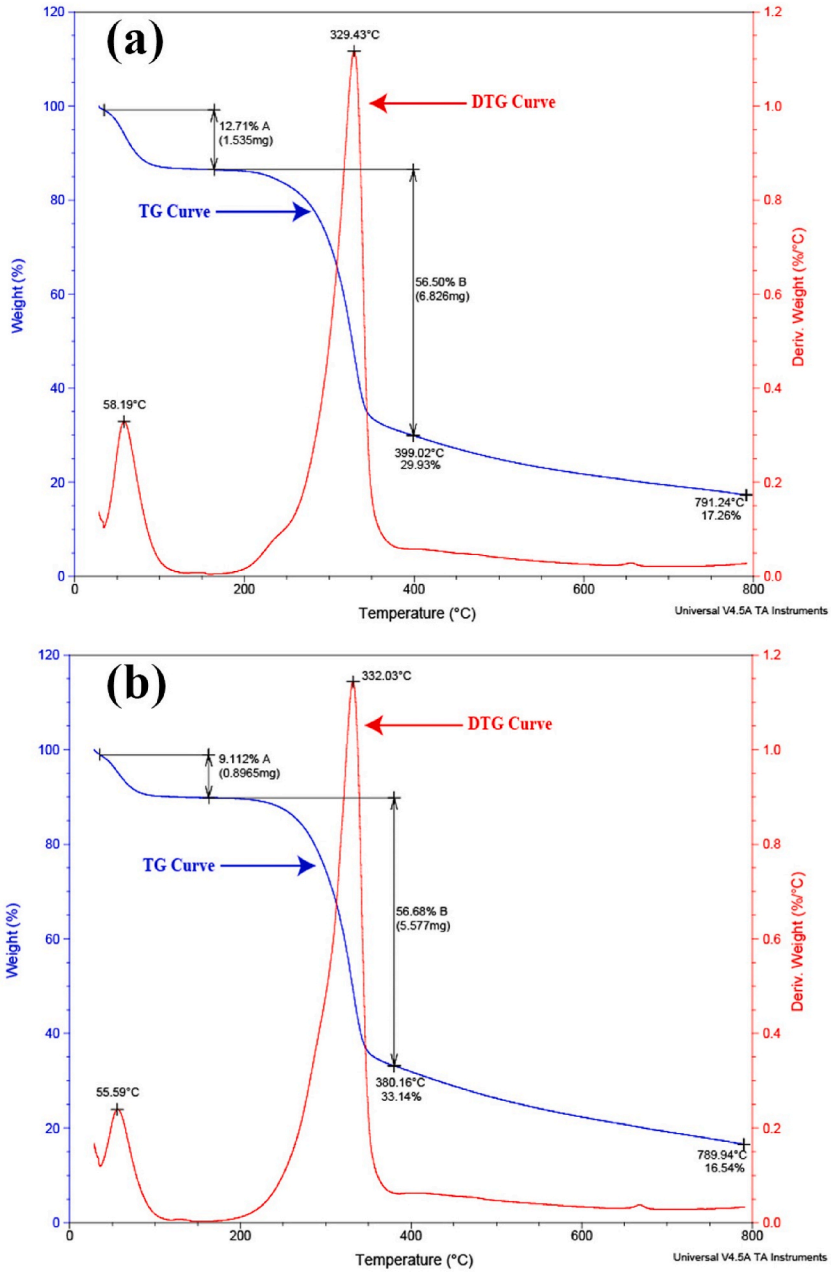

Fig. 9. TG and DTG Curves, (a) LDTF, (b) SGF

of LS fiber was observed with a light reflectance value of 73.79 for LDTF and 73.58 for SGF. The colour strength (K/S) values of LDTF and SGF are 35.9 and 35.8, respectively. These values indicate that the LS fiber requires treatment to improve its dye absorbency in further processing of fibers into textile manufacturing.

The thermogravimetric curves of LS fibers exhibit the thermal stability up to 230 °C confirming that the fiber can withstand most of the textile processing conditions and is possible to be used in the manufacturing of composites.

The outcomes of the fiber characterization investigation, encompassing features like crimped structure, lower count, higher elongation, greater moisture absorbency, satisfactory moisture content, favorable dye absorbency, and good thermal stability, collectively confirm the potential suitability of the LS fiber for the production of biodegradable textile materials. A lower tensile strength and crystalline size of the fibers compared to cotton encourage the end use of biodegradable textiles.

Since the LS plant is known as a herbal plant, as found in the literature review, with all its parts being used in Ayurvedic medicines as a cure for many diseases, there is a possibility to convert fibers to medicinal textiles. Therefore, it is worth investigating the hydrophilicity, nontoxicity and antimicrobial characteristics of the LS rhizome fiber to make decisions about its end use for medicinal

applications. As cellulose fibers are already being used by the pharmaceutical industry to manufacture wound care products and implantable materials for the human body, possibilities are there to utilize the LS plant rhizome fiber for such products too.

Data availability statement

Data included in article/supp. material/referenced in article.

CRediT authorship contribution statement

Methmini Tharanga: Writing – original draft. **Ujithe Gunasekera:** Supervision.

Declaration of competing interest

The authors declare that they have no known competing financial interests or personal relationships that could have appeared to influence the work reported in this paper.

Acknowledgement

The authors wish to thank the Department of Textile and Apparel Engineering, the Department of Material Sciences, the University of Moratuwa, Sri Lanka, and the Sri Lanka Institute of Nanotechnology for their cooperation on this research.

References

[1] T. Toprak, P. Anis, Textile industry's environmental effects and approaching cleaner production and sustainability: an overview, J. Textile Eng. Fashion Technol. 2 (4) (Aug. 2017), https://doi.org/10.15406/jteft.2017.02.00066.
[2] T. Wright, A. Mahmud-Ali, T. Bechtold, Surface coated cellulose fibres as a biobased alternative to functional synthetic fibres, J. Clean. Prod. 275 (Dec. 2020) 123857, https://doi.org/10.1016/j.jclepro.2020.123857.
[3] F. Gapsari, A. Purnowidodo, S. Hidayatullah, S. Suteja, Characterization of Timoho Fiber as a reinforcement in green composite, J. Mater. Res. Technol. 13 (Jul. 2021) 1305–1315, https://doi.org/10.1016/j.jmrt.2021.05.049.
[4] K. Fletcher, Sustainable Fashion and Textiles: Design Journeys, second ed., Routledge, New York, 2012, pp. 11–12.
[5] P. Senthamaraikannan, M. Kathiresan, Characterization of raw and alkali treated new natural cellulosic fiber from Coccinia grandis.L, Carbohydr. Polym. 186 (Apr. 2018) 332–343, https://doi.org/10.1016/j.carbpol.2018.01.072.
[6] M.V. Maheshwaran, N.R.J. Hyness, P. Senthamaraikannan, S.S. Saravanakumar, M.R. Sanjay, Characterization of natural cellulosic fiber from Epipremnum aureum stem, J. Nat. Fibers 15 (6) (Sep. 2017) 789–798, https://doi.org/10.1080/15440478.2017.1364205.
[7] M. Maache, A. Bezazi, S. Amroune, F. Scarpa, A. Dufresne, Characterization of a novel natural cellulosic fiber from Juncus effusus L, Carbohydr. Polym. 171 (Sep. 2017) 163–172, https://doi.org/10.1016/j.carbpol.2017.04.096.
[8] P.G. Baskaran, M. Kathiresan, P. Senthamaraikannan, S.S. Saravanakumar, Characterization of new natural cellulosic fiber from the bark of Dichrostachys Cinerea, J. Nat. Fibers 15 (1) (Apr. 2017) 62–68, https://doi.org/10.1080/15440478.2017.1304314.
[9] Z. Belouadah, A. Ati, M. Rokbi, Characterization of new natural cellulosic fiber from Lygeum spartum L, Carbohydr. Polym. 134 (Dec. 2015) 429–437, https://doi.org/10.1016/j.carbpol.2015.08.024.
[10] R. Kumar, et al., Characterization of new cellulosic fiber from the bark of Acacia nilotica L. Plant, J. Nat. Fibers 19 (1) (Mar. 2020) 199–208, https://doi.org/10.1080/15440478.2020.1738305.
[11] S. Indran, R. Edwin Raj, V.S. Sreenivasan, Characterization of new natural cellulosic fiber from *Cissus quadrangularis* root, Carbohydr. Polym. 110 (Sep. 2014) 423–429, https://doi.org/10.1016/j.carbpol.2014.04.051.
[12] Md Rashid, et al., Natural compounds of lasia spinosa (L.) stem potentiate antidiabetic actions by regulating diabetes and diabetes-related biochemical and cellular indexes, Pharmaceuticals 15 (12) (Nov. 2022) 1466, https://doi.org/10.3390/ph15121466.
[13] P. Hore, B. Tanti, Regeneration of plantlets from rhizome bud explants of lasia spinosa (lour.) thwaites- A medicinal plants of Assam, Int. J. Life Sci. Sci. Res. 4 (3) (May 2018), https://doi.org/10.21276/ijlssr.2018.4.3.1.
[14] A.S.M.A. Reza, et al., Lasia spinosa (L.) thw. attenuates chemically induced behavioral disorders in experimental and computational models, Heliyon 9 (6) (Jun. 2023) e16754, https://doi.org/10.1016/j.heliyon.2023.e16754.
[15] R. Hossain, et al., Lasia spinosa chemical composition and therapeutic potential: a literature-based review, Oxid. Med. Cell. Longev. 2021 (Dec. 2021) 1–12, https://doi.org/10.1155/2021/1602437.
[16] M.K. Dubey, S. Das, S. Yadav, P.C. Gupta, S.K. Jaiswal, B. Sharma, Gastroprotective potential of bioactive fraction from lasia spinosa rhizome on experimentally induced gastric ulceration, Int. J. Pharmaceut. Sci. Res. 5 (12) (2014) 5209–5215, https://doi.org/10.13040/IJPSR.0975-8232.5(12).5209-15.
[17] D. Goshwami, Md M. Rahman, Md A. Muhit, Md S. Islam, M. Anasri, Antioxidant property, cytotoxicity and antimicrobial activity of lasia spinosa leaves, Nepal J. Sci. Technol. 13 (2) (Mar. 2013) 215–218, https://doi.org/10.3126/njst.v13i2.7739.
[18] Md M. Rashid, et al., "Correction: Rashid et al. Natural Compounds of Lasia spinosa (L.) Stem Potentiate Antidiabetic Actions by Regulating Diabetes and Diabetes-Related Biochemical and Cellular Indexes, 2022, Pharmaceuticals 15 (2023) 256, https://doi.org/10.3390/ph16020256, 1466," Pharmaceuticals, vol. 16, no. 2.
[19] T. Kumari, R. Rajapaksha, L. Karunarathne, G. Pushpakumara, P. Bandaranayake, "Morphological characterization of Lasia spinosa (L.) Thw.: screening of indigenous crop genetic resources for future food and nutritional security,", Sri Lanka J. Food Agriculture 3 (2) (Dec. 2017) 29–36, https://doi.org/10.4038/sljfa.v3i2.49.
[20] D. Ariawan, T.S. Rivai, E. Surojo, S. Hidayatulloh, H.I. Akbar, A.R. Prabowo, Effect of alkali treatment of Salacca Zalacca fiber (SZF) on mechanical properties of HDPE composite reinforced with SZF, Alex. Eng. J. 59 (5) (2020, October) 3981–3989, https://doi.org/10.1016/j.aej.2020.07.005.
[21] A.Ç. Kılınç, S. Köktaş, M. Atagür, M.Ö. Seydibeyoglu, Effect of extraction methods on the properties of Althea officinalis L. Fibers, J. Nat. Fibers 15 (3) (Oct. 2017) 325–336, https://doi.org/10.1080/15440478.2017.1325813.
[22] H. Elmoudnia, P. Faria, R. Jalal, M. Waqif, L. Saadi, Effectiveness of alkaline and hydrothermal treatments on cellulosic fibers extracted from the Moroccan Pennisetum Alopecuroides plant: chemical and morphological characterization, Carbohydr. Polymer Technol. Applic. 5 (2023, June) 100276, https://doi.org/10.1016/j.carpta.2022.100276.
[23] L. Segal, J.J. Creely, A.E. Martin, C.M. Conrad, An empirical method for estimating the degree of crystallinity of native cellulose using the X-ray diffractometer, Textil. Res. J. 29 (10) (Oct. 1959) 786–794, https://doi.org/10.1177/004051755902901003.

[24] D. Dai, M. Fan, Investigation of the dislocation of natural fibres by Fourier-transform infrared spectroscopy, Vib. Spectrosc. 55 (2) (Mar. 2011) 300–306, https://doi.org/10.1016/j.vibspec.2010.12.009.
[25] Y. Liu, D. Thibodeaux, J. Rodgers, Preliminary study of linear density, tenacity, and crystallinity of cotton fibers, Fibers 2 (3) (Jul. 2014) 211–220, https://doi.org/10.3390/fib2030211.
[26] I.I. Shuvo, A holistic decision-making approach for identifying influential parameters affecting sustainable production process of canola bast fibres and predicting end-use textile choice using principal component analysis (PCA), Heliyon 7 (2) (Feb. 2021) e06235, https://doi.org/10.1016/j.heliyon.2021.e06235.
[27] N. Baaka, R. Khiari, A. Haji, Ecofriendly dyeing of textile materials with natural colorants from date palm fiber fibrillium, Sustainability 15 (2) (2023, January 16) 1688, https://doi.org/10.3390/su15021688.
[28] M.M. Hasan, K. Abu Nayem, A.Y.M. Anwarul Azim, N.C. Ghosh, Application of purified lawsone as natural dye on cotton and silk fabric, J. Textiles 2015 (2015, April 15) 1–7, https://doi.org/10.1155/2015/932627.
[29] H. A, A.K. Samanta, B. NS, V. PS, S. D, Non-toxic coloration of cotton fabric using non-toxic colorant and nontoxic crosslinker, J. Textil. Sci. Eng. 8 (5) (2018), https://doi.org/10.4172/2165-8064.1000374.
[30] T. Leigh, P. Fernandez-Trillo, Helical polymers for biological and medical applications, Nat. Rev. Chem 4 (6) (2020, May 5) 291–310, https://doi.org/10.1038/s41570-020-0180-5.
[31] V. Fiore, T. Scalici, A. Valenza, Characterization of a new natural fiber from Arundo donax L. as potential reinforcement of polymer composites, Carbohydr. Polym. 106 (Jun. 2014) 77–83, https://doi.org/10.1016/j.carbpol.2014.02.016.
[32] R. Wahab, A. Mohamed, M.T. Mustafa, A. Hassan, Physical characteristics and anatomical properties of cultivated bamboo (bambusa vulgaris schrad.) culms, J. Biol. Sci. 9 (7) (Sep. 2009) 753–759, https://doi.org/10.3923/jbs.2009.753.759.
[33] H. Boumediri, A. Bezazi, G.G. Del Pino, A. Haddad, F. Scarpa, A. Dufresne, Extraction and characterization of vascular bundle and fiber strand from date palm rachis as potential bio-reinforcement in composite, Carbohydr. Polym. 222 (Oct. 2019) 114997, https://doi.org/10.1016/j.carbpol.2019.114997.
[34] K. Subramanian, P. Senthil Kumar, P. Jeyapal, N. Venkatesh, Characterization of ligno-cellulosic seed fibre from Wrightia Tinctoria plant for textile applications—an exploratory investigation, Eur. Polym. J. 41 (4) (Apr. 2005) 853–861, https://doi.org/10.1016/j.eurpolymj.2004.10.037.
[35] J. Jayaramudu, B.R. Guduri, A. Varada Rajulu, Characterization of new natural cellulosic fabric Grewia tilifolia, Carbohydr. Polym. 79 (4) (Mar. 2010) 847–851, https://doi.org/10.1016/j.carbpol.2009.10.046.
[36] A. M. M. A, R. D, S. B. S.R, S.R. P, I. S, D. D, Characterization of natural cellulosic fiber extracted from Grewia damine flowering plant's stem, Int. J. Biol. Macromol. 164 (Dec. 2020) 1246–1255, https://doi.org/10.1016/j.ijbiomac.2020.07.225.
[37] Y. Pan, et al., Structural characteristics and physical properties of lotus fibers obtained from Nelumbo nucifera petiolesc, Carbohydr. Polym. 85 (1) (Apr. 2011) 188–195, https://doi.org/10.1016/j.carbpol.2011.02.013.
[38] D.S. Chen, Y.J. Gan, X.H. Yuan, Research on structure and properties of Lotus fibers, Adv. Mater. Res. 476–478 (Feb. 2012) 1948–1954, 10.4028/www.scientific.net/amr.476-478.1948.
[39] A. Chami Khazraji, S. Robert, Interaction effects between cellulose and water in nanocrystalline and amorphous regions: a novel approach using molecular modeling, J. Nanomater. 2013 (2013) 1–10, https://doi.org/10.1155/2013/409676.
[40] B. NagarajaGanesh, P. Ganeshan, P. Ramshankar, K. Raja, Assessment of natural cellulosic fibers derived from Senna auriculata for making light weight industrial biocomposites, Ind. Crop. Prod. 139 (Nov. 2019) 111546, https://doi.org/10.1016/j.indcrop.2019.111546.
[41] J.E., *Principles of Textile Testing, 3e (PB)* [English], February, CBS Publishers & Distributors, 1996.
[42] R.M.N. Arib, S.M. Sapuan, M.M.H.M. Ahmad, M.T. Paridah, H.M.D.K. Zaman, Mechanical properties of pineapple leaf fibre reinforced polypropylene composites, Mater. Des. 27 (5) (Jan. 2006) 391–396, https://doi.org/10.1016/j.matdes.2004.11.009.
[43] A.C. da Costa Santos, P. Archbold, Suitability of surface-treated flax and hemp fibers for concrete reinforcement, Fibers 10 (11) (Nov. 2022) 101, https://doi.org/10.3390/fib10110101.
[44] M. Daria, L. Krzysztof, M. Jakub, Characteristics of biodegradable textiles used in environmental engineering: a comprehensive review, J. Clean. Prod. 268 (Sep. 2020) 122129, https://doi.org/10.1016/j.jclepro.2020.122129.
[45] E.W. Gaba, B.O. Asimeng, E.E. Kaufmann, S.K. Katu, E.J. Foster, E.K. Tiburu, Mechanical and structural characterization of pineapple leaf fiber, Fibers 9 (8) (Aug. 2021) 51, https://doi.org/10.3390/fib9080051.
[46] D.L. Naik, T.H. Fronk, Weibull distribution analysis of the tensile strength of the kenaf bast fiber, Fibers Polym. 17 (10) (2016, October) 1696–1701, https://doi.org/10.1007/s12221-016-6176-6.
[47] H. M, Imran, Study on color strength of different reactive dyes, J. Textil. Sci. Eng. 7 (2) (2017), https://doi.org/10.4172/2165-8064.1000293.
[48] K. Murugesh Babu, M. Selvadass, R. Somashekar, Characterization of the conventional and organic cotton fibres, J. Textil. Inst. 104 (10) (Oct. 2013) 1101–1112, https://doi.org/10.1080/00405000.2013.774948.